Mucosal Immunology
nature publishing group

Pulmonary immunization with a recombinant Influenza A virus vaccine induces lung-resident CD4$^+$ memory T cells that mediate protection against tuberculosis

Journal:	*Mucosal Immunology*
Manuscript ID	MI-18-052
Manuscript Type:	Article
Date Submitted by the Author:	15-Feb-2018
Complete List of Authors:	Flórido, Manuela; Centenary Institute, Tuberculosis Research Program Muflihah, Heni; Centenary Institute, Tuberculosis Program Lin, Leon; Centenary Institute, Tuberculosis Program Xia, Yingju; Deakin University, School of Medicine Sierro, Frederic; Centenary Institute, Liver Immunology Program; University of Sydney Sydney Medical School, Pathology Palendira, Mainthan; Centenary Institute, Tuberculosis Program Feng, Carl; Centenary Institute, Tuberculosis Program; University of Sydney, Infectious Diseases and Immunology Bertolino, Patrick; Centenary Institute, Tuberculosis Program; Royal Prince Alfred Hospital, AWMorrow Gastroenterology and Liver Center Stambas, John; Deakin University, School of Medicine Triccas, James; Centenary Institute, Tuberculosis Research Program; University of Sydney Sydney Medical School, Infectious Diseases and Immunology Britton, Warwick; Centenary Institute, Tuberculosis Program; The University of Sydney, Sydney Medical School and the Marie Bashir Institute for Infectious Diseases and Biosecurity
Keyword:	vaccine, resident memory, lung, protection
Please identify up to three subject search terms that best define your manuscript.:	T cells < Cells, Pulmonary tract < Tissues, Infectious < Disease

Note: The following files were submitted by the author for peer review, but cannot be converted to PDF. You must view these files (e.g. movies) online.

supplementary video1.mov
supplementary video2.mov

Pulmonary immunization with a recombinant Influenza A virus vaccine induces lung-resident CD4$^+$ memory T cells that mediate protection against tuberculosis

Manuela Flórido[1], Heni Muflihah[1], Leon C.W. Lin[1], Yingju Xia[2], Frederic Sierro[3,7], Mainthan Palendira[1], Carl G. Feng [5], Patrick Bertolino[3,4], John Stambas[2] , James A. Triccas[1,5] and Warwick J. Britton[1,5,6]

[1]Tuberculosis Research Program, and [3]Liver Immunology Program, Centenary Institute, University of Sydney, Newtown, NSW, Australia

[2]School of Medicine, Deakin University, Geelong, VIC, Australia

[4]AWMorrow Gastroenterology and Liver Centre, Royal Prince Alfred Hospital, Camperdown, NSW, Australia.

[5]Department of Infectious Diseases and Immunology, and [6]Department of Medicine, Sydney Medical School, University of Sydney, NSW, Australia.

[7]Department of Pathology, Sydney Medical School, University of Sydney, NSW, Australia.

Key Words: Recombinant Influenza A virus, mycobacteria, lung, T cells, protection, tissue resident memory cells

Corresponding author: Warwick Britton

[1]Tuberculosis Research Program, Centenary Institute, Locked Bag No. 6, Newtown, NSW 2042. Australia.

Email: w.britton@centenary.org.au

Telephone: 61-2-9515 5210

Facsimile: 61-2-9565 6110

Abstract

The lung is the primary site of infection with the major human pathogen, *Mycobacterium tuberculosis*. Effective vaccines against *M. tuberculosis* must stimulate memory T cells to provide early protection in the lung. Recently, tissue resident memory T cells (T_{RM}) were found to be phenotypically and transcriptional distinct from circulating memory T cells. Here, we identified *M. tuberculosis*-specific $CD4^+$ T cells induced by recombinant influenza A viruses (rIAV) vaccines expressing *M. tuberculosis* peptides that persisted in the lung parenchyma with the phenotypic and transcriptional characteristics of T_{RM}s. To determine if these rIAV-induced $CD4^+$ T_{RM} were protective independent of circulating memory T cells, mice previously immunized with the rIAV vaccine were treated with the sphingosine-1-phosphate receptor modulator, FTY720, prior to and during the first 17 days of *M. tuberculosis* challenge. This markedly reduced circulating T cells, but had no effect on the frequency of *M. tuberculosis*-specific $CD4^+$ T_{RM}s in the lung parenchyma or their cytokine response to infection. Importantly, mice immunized with the rIAV vaccine were protected against *M. tuberculosis* infection even when circulating T cells were profoundly depleted by the treatment. Therefore, pulmonary immunization with the rIAV vaccine stimulates lung-resident $CD4^+$ memory T cells that confer early protection against tuberculosis infection.

Introduction

Tuberculosis (TB) is the major cause of death from a bacterial pathogen in adults worldwide; in 2016 alone there were 1.6 million deaths and an estimated 10.4 million new cases[1]. The current vaccine, BCG, although able to protect children from disseminated infection, fails to protect the adults from the contagious pulmonary form of disease[2]. The protective immune response against *M. tuberculosis* is mostly dependent on $CD4^+$ T cells[3] as evidenced by the increased susceptibility of individuals with HIV/AIDS to TB[4]. Novel TB vaccines that induce T cells are being actively pursued, but so far with limited success[5], suggesting that new strategies are required

Until recently, memory T cells were considered to exist as two main subsets that exclusively circulated from the blood into tissues or lymphoid organs. While central memory T cells (T_{CM}) are able to enter lymphoid organs, effector memory T cells (T_{EM}) circulate through peripheral sites. The observation that subsets of virus-specific long-lived $CD8^+$ T memory cells were located in non-lymphoid tissues[6] suggested the existence of non-circulating populations of tissue-resident memory T cells (T_{RM}). Their tissue residence was subsequently confirmed by parabiosis studies[7].

T_{RM} found in several tissues, including the lung[6], are phenotypically and functionally distinct from their circulating T_{CM} and T_{EM} memory T cell counterparts. They express low levels of the transcription factor, Kruppel-like factor 2 (KLF2), and spinghosine-1-phosphate (S1P) receptor, S1PR1, and high levels of C-type lectin, CD69[8]. Expression of S1PR1 and its regulatory transcription factor KLF2 are essential for promoting T lymphocyte egress into circulation[9,10]. Downregulation of these two genes in T_{RM} prevent them from sensing the S1P gradient in the circulation[11], thus inhibiting their exit from tissues.

The presence of T_{RM} in tissues has been associated with protection against several pathogens, and the high number of T_{RM} found in mucosal sites support the concept that these cells represent a first line of defence against pathogens[8]. Most studies have focused on $CD8^+$ T_{RM} cells in the context of viral infections and demonstrated these cells can protect mice against viruses[12-14], *Listeria monocytogenes*[15] and malaria[16]. The induction of $CD4^+$ T_{RM} cells has been less studied but growing evidence of the presence and protective function of these cells, particularly in the lung, is emerging[17-19].

We have previously shown that pulmonary immunization of mice with a viral TB vaccine, recombinant influenza A virus (rIAV) expressing the p25 $CD4^+$ T cell immunodominant epitope of *M. tuberculosis* Ag85B (PR8.p25), induced strong p25-specific $CD4^+$ T cell responses in the lungs that were protective against *M. tuberculosis* challenge[20]. In this study we have investigated whether pulmonary immunization of mice with rIAVs expressing this p25 epitope induces *M. tuberculosis*-specific $CD4^+$ T cells in the lung with the tissue location, phenotype and transcriptional characteristics of T_{RM}s and if these lung-resident T cells are protective against *M. tuberculosis* challenge in the absence of circulating memory T cells.

Results

Pulmonary, but not systemic, immunization with PR8.p25 induces P25 $CD4^+$ T cells in the lung

To determine if mucosal immunization with PR8.p25 is required for the induction of the P25-specific $CD4^+$ T cell response in the lungs, $5x10^4$ $CD45.1^+$ P25 cells, expressing a transgenic TCR recognizing the p25 $CD4^+$ T cell epitope of the *M. tuberculosis* Ag85B, were transferred intravenously (i.v.) into C57BL/6 mice that

were infected on the following day, either intranasally with 20 pfu or intraperitoneally (i.p.) with 10^4 pfu of PR8.p25. Three weeks later, the P25-specific response was measured in the lung and spleen by IFN-γ ELISpot and flow cytometry. Intranasal infection with PR8.p25 led to strong responses to both the *M. tuberculosis*-specific p25 epitope $Ag85B_{240-254}$ and the IAV endogenous $CD8^+$ T cell epitope, $NP_{366-374}$, in both the lung (Fig 1A) and spleen (Fig 1B). Intraperitoneal infection with PR8.p25 induced splenic T cell responses that were comparable to those induced by intranasal immunization, but failed to induce substantial responses in the lungs. These findings were confirmed by flow cytometry as significant numbers of P25 transgenic cells were present in the broncho-alveolar lavage (BAL) and total lung cell suspensions only when mice were infected intranasally with PR8.p25 (Fig 1C and D). By contrast, similar numbers of P25 donor T cells were found in the spleen after infection by either route (Fig 1E). These results demonstrate that optimal generation of a p25-specific $CD4^+$ T cell response in the lungs requires the pulmonary delivery of the vaccine.

Intranasal immunization with PR8.p25 leads to the persistence of $CD69^+CD11a^+$ $CD44^{hi}CD62L^{lo}$ P25 $CD4^+$ T cells in the lung

The kinetics of the $CD4^+$ T cell response were monitored after adoptive transfer of P25 cells and intranasal immunization with PR8.p25. The p25-specific $CD4^+$ T cells response in the lungs underwent a robust expansion 2 weeks after immunization. At 6 weeks post immunization after contraction of the response, a significant number of p25-specific cells ($2x10^4$) was detected in the lungs (Fig 2A). The majority of these persisting P25 $CD4^+$ T cells expressed CD69, but less than 5% expressed CD103 (Fig 2B). Of note, the proportion of P25 $CD4^+$ T cells expressing CD69 increased

following infection and by week 8 post infection more than 90% of the P25 $CD4^+$ T cells in the lung were $CD69^+$ (Fig 2C). CD69 expression in the persistent P25 $CD4^+$ T cells was not due to recent activation caused by antigen remaining in the lungs. This was confirmed by the failure of CFSE-labelled P25 transgenic CD45.1+ $CD4^+$ T cells to proliferate in the lungs and lymph nodes when adoptively transferred into mice 6 weeks after immunization with PR8.p25. By contrast, CFSE-labelled P25 T cells proliferated when transferred 5 days after immunization (Fig S3).

To assess whether P25 $CD4^+$ T cells persisting in the lung at 8 weeks after immunization were located in the tissue or in the vasculature, mice were injected iv with anti-CD45 antibodies 3 minutes prior to harvesting of the lungs as described[21]. The vast majority (>95%) of the lung P25 $CD4^+$ T cells failed to be stained by anti-CD45 antibodies, indicating they were located in the lung parenchyma (Fig 2C). Parenchymal, CD45-unlabelled P25 $CD4^+$ T cells expressed CD69, in contrast to circulating, CD45-labelled P25 $CD4^+$ T cells that did not express this marker (Fig 2D), Similar low levels of CD69 expression were observed in CD45-labelled $CD3^+CD4^+$ T cells present in the lung vasculature (Fig S1). Further, phenotypic analysis showed that the majority of P25 $CD4^+$ T cells retained in the lung parenchyma at 8 weeks after immunization with PR8.P25 expressed both CD69 and CD11a (Fig 2E and G) and were $CD44^{hi}CD62L^{lo}$ (Fig 2F).

P25 $CD4^+$ T cells induced by immunization with PR8-p25 are distributed throughout the lung parenchyma

To determine the *in situ* localization of the P25 $CD4^+$ T cells following the rIAV immunization, 2-photon microscopy was performed on the lungs collected from

immunized mice. Consistent with flow cytometry results, imaging using 2-photon microscopy showed that at 8 weeks after intranasal PR8.p25 infection, P25 T cells expressing GFP (P25-GFP) were readily detectable in the lungs (Fig 3A). The extra-vascular location of these P25-GFP cells was confirmed by imaging the lungs of infected mice in which the vessels were labelled with fluorescent wheat germ agglutinin (Fig 3B, Supplementary video1). Furthermore, clearing of the lungs with RapiClear1.52 solution allowing deeper imaging of tissue revealed that the P25-GFP cells were scattered throughout the lung, from the pleura to the more central areas near the airways (Fig 3C, Supplementary video 2). Quantification of the P25-GFP cells present in the lungs after 8 weeks of PR8.p25 immunization using 2-photon randomly acquired z-stacks showed that the density of these cells was 17-224 cells/mm^3 of lung, 57-75 times more that what determined by flow cytometry for the lungs of the same mice (Fig 3D). Strikingly, 36 weeks after pulmonary immunization of PR8.p25, parenchymal $CD69^+CD11a^+$ P25 $CD4^+$ T cells were still detected in the lungs of all the mice analysed, with a mean number of 133 ±111 (±SD, n=7). Thus, immunization with PR8.p25 leads to long-term persistence of $CD62L^{lo}CD44^{hi}CD69^+CD11a^+$ P25 $CD4^+$ memory T cells in the lung parenchyma.

P25 $CD4^+$ T cells induced by PR8.p25 immunization have the transcriptional signature of TRMs

To investigate further the properties of the vaccine-induced memory T cells, lung and splenic P25 T cells from mice immunized intranasally with PR8.p25 six weeks earlier were sorted according to their memory phenotype, and the transcriptional profiles of naïve, effector and the different memory P25 cell subsets were analyzed by qPCR. Lung $CD69^+$ P25 cells displayed a distinct reduction in Klf2 and S1pr1 mRNA levels

compared to their splenic CD69^{-}CD62L^{lo} counterparts (Figure 4A). The transcription of FOXO1, an upstream regulator of KLF2[22], was also more markedly downregulated in the lung CD69^{+} memory T cells than in splenic memory T cells. Lung CD69^{+} memory P25 cells also expressed higher levels of *Tbx21* and *Ifng* mRNA and higher levels of pro-survival markers, *Bcl2* and *Bclxl* than splenic effector memory CD4 T_{EM} (Figure 4A, B). There results demonstrate that the long-lived, pulmonary *M. tuberculosis*-specific CD4^{+} T cells induced by pulmonary immunization with PR8.P25 exhibit the transcriptional profile of tissue resident memory T cells

The persistence of P25 CD4^{+} T cells induced by rIAV immunization in the lung is independent of replenishment of circulating T cells

To test if the rIAV-induced P25 CD4^{+} T cells residing in the lung parenchyma were dependent on the continuing recruitment of circulating CD4^{+} T cells, the response to PR8.p25 was examined in mice with lymphopenia following administration of FTY720, a S1P receptor modulator that inhibits egress of lymphocytes from lymph nodes and other secondary lymphoid organs[23,24]. Six weeks after immunization with PR8.p25, mice were administered i.p. 1 mg/kg of FTY720 or PBS daily for 20 days. The treatment with FTY720 significantly reduced the percentage of circulating CD3^{+}CD4^{+} T cells both in the peripheral blood and in the lung vasculature, but did not affect the number of P25 CD69^{+}CD4^{+} T cells in the lung parenchyma (Fig S4). This demonstrated that the P25 CD4^{+} T cells present in the lung parenchyma six weeks after PR8.p25 immunization were non-circulating memory T cells that persisted in the tissue without requiring replenishment from by circulating cells. We then used this model to assess the response of rIAV-induced CD4^{+} T_{RM} cells against challenge with *M. tuberculosis*. B6 mice were immunized with rIAV X31.p25 vaccine

197 that encodes the same *M. tuberculosis* p25 epitope and stimulates lung $CD4^+$ T_{RM}
198 cells that protect mice against *M. tuberculosis* infection (Muflihah et al, unpublished).
199 Three days after FTY720 treatment both immunized and non-immunized mice were
200 challenged by aerosol infection with low dose *M. tuberculosis*. The $CD4^+$ T responses
201 to infection in FTY720-treated versus non-treated mice were assessed on 17 and 28
202 days post-infection (dpi) (Fig 5A). As expected FTY720 treatment led to significant
203 reduction in the number of circulating $CD4^+$ T cells in both immunized and
204 unimmunized mice at 17 dpi (Fig 5B). Similar effects were also seen in the MLN (Fig
205 5C), lung parenchyma (Fig 5D and S5) and lung vasculature (Fig 5E and Fig S5). At
206 28 dpi, 11 days after terminating FTY720 treatment, the number of cells was similar
207 in all experimental groups (Fig S6). There was a small decrease in the number of
208 donor P25 $CD4^+$ T cells present in the lung parenchyma of the treated mice at day 17
209 dpi (Fig 5 F) suggesting that at this time-point after *M. tuberculosis* challenge there
210 was recruitment of circulating GFP-p25 cells in to the lung. Importantly, the GFP-P25
211 population with the T_{RM} signature ($CD11a^+CD62L^{lo}CD69^+KLRG^{-}$) was still the most
212 abundant subset in the lung parenchyma of the immunized mice (Fig 5 G) and the
213 number of these cells was not affected by FTY720 treatment (Fig 5 H). Thus, the T_{RM}
214 $CD4^+$ T cells induced by rIAV vaccines were maintained in the lungs independently
215 of circulating T cells.
216
217 ***The $CD4^+$ T_{RM}s induced by rIAV immunization produce Th1 cytokines in response***
218 ***to M. tuberculosis challenge***
219 The cytokine production in the lungs of the immunized and unimmunized mice, with
220 or without FTY720 treatment, was analysed at 17 and 28 dpi by ICS after incubation
221 of cells in the presence of p25 peptide. At 17 dpi, both groups of mice immunized

with the rIAV vaccine had significantly higher magnitude of $CD4^+$ T cell cytokine responses than the unimmunized groups, particularly triple-cytokine (IFNγ/TNFIL-2) producers and double (IFNγ/TNF) producers (Fig 6A). The majority of the cytokine producing T cells was located in the lung parenchyma (Fig S6) and corresponded to donor GFP-P25 $CD4^+$ T cells (Fig 6B). FTY720 treatment had no effect on the cytokine production by GFP-P25 $CD4^+$ T cells at any time point (Figs 6B and 6C). At 28 dpi the cytokine profile changed into a more effector phenotype consisting of IFNγ or IFNγ/TNF production by donor GFP-P25 $CD4^+$ T cells (Fig 6C) and other p25-specific $CD4^+$ T cells without significant differences between groups (Fig S7). Therefore, the T_{RM} $CD4^+$ T cells induced by rIAV vaccines were able to produce macrophage-activating cytokines in response to *M. tuberculosis* challenge.

The $CD4^+$ T_{RM}s induced by rIAV immunization are protective against M. tuberculosis in the lung

To determine if the $CD4^+$ TRMs induced by the rIAV vaccination protected mice against *M. tuberculosis*, the mycobacterial loads contained in the lungs of immunized and non-immunized mice with or without FTY720 treatment were determined at 17 and 28 days after aerosol challenge (Fig 5A). At 17 dpi, rIAV vaccination conferred significant protection in the lung. More importantly, the vaccine-induced responses were protective in FTY720-treated mice (Fig 7A), in which the circulating $CD4^+$ T cells were substantially depleted (Fig 5A). At 28 dpi, unimmunized mice treated with FTY720 showed a trend towards higher bacterial loads compared to the non-treated unimmunized mice (Fig 7B). Although there were no differences in the number of $CD4^+$ T cells at 28 dpi between groups (Fig S6) this enhanced susceptibility to

infection may be due to a delay in the recruitment of cells to the lung caused by the FTY720 treatment. Strikingly, this effect was absent in mice that were immunized with the rIAV vaccine (Fig 7B), demonstrating that the presence of lung T_{RM}s induced by the rIAV vaccine not only conferred protection, but also limited the increased susceptibility to *M. tuberculosis* infection induced by prior FTY720 treatment.

Discussion

There is growing interest in developing vaccines that are able to induce tissue resident memory cells at the site of subsequent infection. This is particularly relevant for TB vaccines since direct recognition of infected macrophages by $CD4^+$ T cells is required for protection against *M. tuberculosis*[25], and there is evidence that *M. tuberculosis*-specific $CD4^+$ T cells that localize in the lung parenchyma have greater capacity to control infection than $CD4^+$ T cells present in the vasculature[26]. Furthermore the protective efficacy of mucosal-delivered BCG vaccination has been associated with the development of lung resident $CD4^+$ T cells[27,28]. Because of their location in the mucosal tissues pathogen-specific $CD4^+$ T_{RM} are considered to be the first line of defence, providing a timely *in situ* response that can help recruit other immune cells to the site of infection[29].

In this work, we demonstrated that immunization of mice with a rIAV-vectored TB vaccine led to the long-term retention of *M. tuberculosis*-specific tissue resident memory $CD4^+$ T cells in the lung. This is dependent on mucosal immunization since immunization by the i.p. route with the PR8.p25 vaccine failed to significantly induce such responses. This is consistent with the fact that intranasal, but not parenteral,

immunization with BCG was necessary to induce T cell responses in the airway luminal compartment[30]. Similarly, Perdomo *et al* showed that intratracheal vaccination with BCG induced significantly higher numbers of $CD4^+$ and $CD8^+$ T cells to the airways subcutaneous immunization[28].

The P25 $CD4^+$ T cells present in the lung parenchyma of the mice immunized by PR8.p25 exhibited the phenotype associated with tissue resident memory T cells , namely expression of CD69 in the absence of recent antigen stimulation. Of note, the $CD4^+$ memory T cells induced in the lung by the PR8.p25 vaccine did not express the marker CD103, commonly co-expressed with CD69 in $CD8^+$ T_{RM} cells in some tissues[31]. The rIAV-induced P25 $CD4^+$ T_{RM} cells expressed high levels of CD11a which is also present on parenchymal $CD4^+$ memory T cells that develop after respiratory virus[32] and bacterial[26] infections. The P25 $CD4^+$ cells were scattered throughout the lung, from areas close to the pleura to those adjacent to the more central airways and blood vessels, consistent with their putative role as the first line of defence at the site of infection. Furthermore, the fact that the persistence of these cells was not affected by FTY720-induced lymphopenia is a strong indication that these are indeed long-lived tissue resident memory cells that do not circulate through lymphoid organs and are not dependent on replenishment by circulating cells.

The $CD69^+$ P25 cells persisting in the lungs 6 weeks after immunization with PR8.p25 showed a typical transcriptional profile associated with tissue residency, with downregulation of Klf2 and S1p1r genes[33,34]. Interestingly the upstream regulator gene Foxo1 was only modestly downregulated in the lung $CD69^+$ P25 cells, and this may be due to this gene being regulated by non-transcriptional mechanisms,

297 such as phosphorylation and ubiquitination[35]. Together with the high levels of
298 expression of the pro-survival markers, Bcl-2 and Bcl-xL, these data indicate that the
299 rIAV vaccine-induced CD69$^+$ P25 cells can establish a long-term residency in the
300 lungs of immunized mice.
301 Strikingly the enumeration of P25 T cells in digested lungs using flow cytometry was
302 a gross underestimate (average 66 times less) of the total number of P25 T cells
303 identified by 2-Photon microscopy. These results are in close concordance with
304 previous report that detected 69-fold more pathogen-specific CD8$^+$ memory T cells by
305 quantitative immunofluorescence microscopy, compared to flow cytometry in the
306 lungs of mice infected with LCMV[7]. Considering that the loss of cells by digestion of
307 the lungs may affect the resident cell population more than circulating cells, these
308 results reinforce the notion that studies on tissue resident memory cells will benefit
309 greatly from including imaging of the cleared tissues to provide a more reliable
310 quantification of T cells and their location. Nevertheless, in spite of the
311 underestimation determined by flow cytometry, we found that P25 specific CD4$^+$ T
312 cells induced by the rIAV vaccine were retained in the lung parenchyma at higher
313 numbers than those generated by pulmonary deliver of BCG[28]. This can be related to
314 the adoptive transfer strategy used in this study. Nevertheless, we obtained similar
315 numbers of P25 CD4$^+$ T_{RM} cells in the lungs 6 weeks after immunization with
316 PR8.p25 regardless of whether the adoptive transfer was performed using 10^4 or 400
317 P25 cells (data not shown). suggesting that the generation of T_{RM}s may be more
318 dependent on the quality of the effector immune response generated than on the
319 number of precursors present at the time of immunization. In addition, these P25 T_{RM}
320 CD4$^+$ T cells were still detected 36 weeks after rIAV immunization, longer than
321 described for other models of infection[28]. Furthermore, the lung CD69$^+$ memory p25

cell subset that persisted after PR8.p25 immunization had higher levels of Tbx21 and Ifng mRNA expression than the splenic T_{EM} cells. This elevated expression of Th1-associated genes indicates these lung-resident $CD69^+$ memory T cells are poised for cytokine production upon recall at the mucosal sites and therefore likely to contribute with faster and stronger protective immune responses against future pulmonary infection. In fact, after challenge with *M. tuberculosis* the parenchymal P25 $CD4^+$ T_{RM} cells induced by immunization with rIAV vaccine produced polyfunctional cytokine responses much earlier than the P25 $CD4^+$ T cells generated by the *M. tuberculosis* even when circulating $CD4^+$ T cells were substantially depleted by FTY720 treatment. This is in concordance with previous study using FTY720 that showed that memory T cells present in the lungs following BCG immunization were sufficient to protect mice from a subsequent BCG challenge[27] and with report by Sakai and colleagues showing that *M. tuberculosis*-specific $CD4^+$ T cells isolated from the lung parenchyma were more protective against subsequent *M. tuberculosis* challenge than their counterparts from the lung vasculature when adoptively transferred into naïve $TCRa^{-/-}$ mice[26]. In our study, not only the P25 $CD4^+$ T_{RM}s induced by the rIAV vaccine showed early protection against challenge in the absence of circulating cells, but also were also able to overcome the increased susceptibility to infection owing to the delayed $CD4^+$ T cell response caused by previous FTY720 treatment. These results strengthen the idea that developing vaccines with maximum potential to induce T_{RM} populations at the sites of infection may be more effective than those inducing merely high circulating memory responses.

In a recent study assessing the ability of currently licenced influenza vaccines ability to generate T_{RM}, intranasal administration of live attenuated influenza A virus (Flu

Mist) induced virus-specific $CD4^+$ and $CD8^+$ T_{RM} cells in the lungs, while the injectable, inactivated vaccine Fluzone or the live attenuated vaccine given by the intraperitoneal or sub-cutaneous routes induced mainly strain–specific neutralizing antibodies[36]. Furthermore intranasal delivery of the inactivated vaccine failed to generate the increased $CD3^+CD69^+$ memory T cells observed in the lungs after the immunization with the live attenuated vaccine. These results indicate that the ability to provide long-term protection against vaccine and non-vaccine viral strains in mice is linked to the establishment of a stable population of long-term T_{RM} cells by targeting the respiratory track with live attenuated viruses.

Another influenza A virus-based TB vaccine, TB/FLU-04L (Research Institute for Biological Safety Problems, Kazakhstan), has been developed, completed a phase I and is currently in a phase II clinical trial. This replication-deficient influenza vector, which expresses the *M. tuberculosis*-specific proteins ESAT6 and Ag85A, was well tolerated when administered by the intranasal route and induced nasal antigen-specific $CD4^+$ and $CD8^+$ T cell responses[37]. Here we have shown that a rIAV TB vaccine that induces a potent immune $CD4^+$ T cell response to the *M. tuberculosis* antigen generated a long-lasting population of *M. tuberculosis*-specific $CD4^+$ T_{RM}s in the lungs of the immunized mice, which readily produce cytokines in response to *M. tuberculosis* challenge and confer significant protection in the lung. Therefore the use of live attenuated rIAV–based TB vaccines may be an attractive vaccine strategy, either as primary pulmonary vaccine or to boost BCG in order to stimulate long-lasting T_{RM} cells in the lungs that can respond *in situ* as the first line of defence against pulmonary *M. tuberculosis* infection.

Methods

Influenza recombinant virus

DNA encoding the *M. tuberculosis* Ag85B(Rv1886c)$_{240\text{-}254}$ CD4$^+$ T cell epitope (FQDAYNAAGGHNAVF, p25) was inserted into the neuraminidase (NA) stalk of the H1N1 PR8 influenza virus between amino acids 43 and 44[20]. rIAV PR8.p25 was generated using an eight-plasmid reverse genetics system, as previously described[38]. Briefly, 1 μg of 8 pHW2000 DNA plasmids containing each influenza gene segment, including the pHW2000 plasmid encoding the genetically modified NA segment, were transfected into a co-culture of human embryonic kidney 293 (HEK293T) cells and Madin–Darby canine kidney cells (MDCK). Viruses were then injected into 10-day-old embryonated eggs, and after 48 hr incubation, recombinant viruses were harvested from the allantoic fluid and virus titres determined using a plaque assay[39]. The presence of recombinant virus was determined using a hemagglutination assay, and insertion of the appropriate epitopes was confirmed by sequencing.

Mice

Six to eight week old female C57BL/6 were purchased from the Australian BioResources (NSW, Australia). P25 CD4$^+$ TCR transgenic mice (specific for residues 240-254 of *M. tuberculosis* Ag85B) were kindly provided Dr. J Ernst (New York University, NY). P25 CD4$^+$ TCR transgenic mice expressing both the *M. tuberculosis* p25 epitope and GFP under the control of the Ubiquitin promoter (P25-GFP) were kindly provided by Prof WR Heath (Peter Doherty Institute, University of Melbourne, Australia). The mice were maintained in specific pathogen–free conditions and bred at Centenary Institute. All mouse experiments were approved by the Sydney Local Health District Animal Ethics Committee.

397

398 Mouse immunizations, treatments and infection

399 $5x10^4$ P25 Tg or P25-GFP cells were transferred by i.v. injection into recipient
400 C57BL/6 mice one day prior to immunization. Mice were infected intranasally with
401 20 pfu of PR8.p25 or 10^4 pfu of X31.p25 and wild type IAVs in 50 µl of saline
402 solution. In some experiments 10^4 pfu PR8.p25 were injected i.p in a volume of 200
403 µl of saline solution. Intravascular staining was performed by injecting mice i.v. with
404 5 µg of APC-Cy7-conjugated rat anti-mouse CD45 antibody 3-5 minutes before being
405 euthanized.
406 FTY720 (Sigma) was administered by i.p., 1 mg/kg in PBS, daily for 20 days. To
407 assess the protective efficacy of the vaccines the mice were challenged with 100 cfu
408 of *M. tuberculosis* H37Rv using a Middlebrook airborne infection apparatus[20] (Glas-
409 Col, IN, US).

410

411 Lung and spleen processing

412 Lungs were digested in RPMI/10%FCS containing collagenase IV at 100 U/ml and
413 DNase I at 25 µg/ml for 30 min at 37°C. Spleens were disrupted by passage through
414 70 µm cell strainers and washed with RPMI/10% Fetal calf serum (FCS). Lung and
415 spleen cell suspensions were incubated with 1 ml of ACK lysis buffer for 2 minutes to
416 remove red blood cells, washed and resuspended in appropriate volume of
417 RPMI/10%FCS.

418

419 IFNγ ELISpot

420 Cells were cultured at a density of less than $2x10^6$ cells/ml of RPMI/10%FCS in an
421 ELISpot plate pre-coated with 15 µg/ml of anti-mouse IFNγ monoclonal antibody

(clone AN18) in the presence of pathogen-specific peptides, $NP_{366-374}$ and $Ag85B_{240-254}$ (Genscript), at a final concentration of 10 µg/ml or with BCG lysate at a final concentration of 5 µg/ml. As controls, cells were incubated with media alone. After 18 hr of incubation plates were thoroughly washed with PBS/0.01%Tween20 and incubated with biotinylated anti-mouse IFNγ monoclonal antibody (clone XMG1.2) at final concentration 2.5 µg/ml for 2 hr at 37C. Development was achieved by incubation with avidin-conjugated alkaline phosphatase (Sigma) followed by addition of AP conjugate substrate (Biorad). The numbers of spots were determined using an AID ELISpot Reader.

Flow cytometry

Two million cells were incubated with 1.25 µg/ml of anti-CD32/CD16 (eBiosciences) in FACS wash buffer (PBS/2%FCS/0.1%NaN3) for 30 min to block Fc receptors, washed and incubated for 30 min with a mix of fluorescent antibodies. The following antibodies were used: PerCPCy5.5-CD3 (BD Biosciences), Alexa700-CD4 (BD Biosciences), PE-CD69 (BD Biosciences), efluor450-CD62L (BD Biosciences), FITC-CD44 (Biolegend), PECy7-KLRG1 (BD Biosciences) and BV510-CD11a (BD Biosciences). Blue fixable cell death stain (Invitrogen) was added to the antibody mix at dilution recommended by manufacturer to allow dead cell discrimination. Surface markers were analyzed using the gating strategy described in Supporting Figure S1 and FlowJo Bolean gating tool.

For intracellular staining $4x10^6$ spleen cells were incubated overnight in the presence of 10 µg/ml of $Ag85B_{240-254}$ peptide (Genscript), and 4 h prior to collection 10 µg/ml of BrefeldinA was added to each well. Cells were stained with anti-CD3, anti-CD4 antibodies and blue fixable cell death stain, fixed and permeabilized with

Cytofix/Cytoperm (BD Biosciences) prior to staining with anti-cytokine antibodies (PECy7-IFNγ, APC-TNF and BV510-IL2, BD Biosciences) for 20 min. Cells were then washed with Permwash (BD Biosciences) and resuspended in FACS buffer. Cytokine expression was analyzed using the gating strategy described in Supporting Figure S2 and FlowJo Bolean gating tool.

Samples were run on a LSR Fortessa Flow cytometer. Analysis was performed using FlowJo software (TreeStar, Ashland, OR)

Lung clarification and two photon microscopy

Lungs were fixed with 10% formalin and cleared for at least 12 hours with RapiClear1.52 (Sunjilab, Taiwan). The cleared lungs were mounted into slides fitted with iSpacers (Sunjilab, Taiwan) filled with the clearing reagent before analysis using a Nikon Ti-U inverted fluorescence microscope with a 25x Nikon water immersion objective (1.1 NA, WD 2 mm) and a dedicated single-beam LaVision TriM Scope I (LaVision Biotec: Germany) controlled by Imspector software (LaVision). The microscope was outfitted with one Ti:Sapphire laser (MaiTai DeepSee: Spectra-physics) and one Synchronously Pumped Optical Parametric Oscillator (OPO) pumped by a Chameleon Ultra II Ti:Sapphire laser (Coherent). Emission wavelengths were collected with ultrasensitive photomultiplier tubes (GaSP Hamamatsu) for 412-472 nm (second harmonic signal), 490-520 nm (GFP), 573-633 nm (A594). The DeepSee laser was tuned to 940 nm and OPO was tuned to 1080nm. Parfocal alignment of lasers was adjusted using fluorescent beads before each experimental session. Data correction and analysis were conducted using ImarisJ software (Bitplane, South Windsor, CT). For detection of vascular vessels mice were injected i.v. with Alexa 594-conjugated wheat germ agglutinin 30 minutes prior to organ collection.

For quantification of GFP positive cells in the lungs, 2 µm step z-stacks of 400 µm x 400 µm x 1200 µm random areas of the right lobes were acquired. Quantification was done using the Imaris11 spot tool based on at least 7 random z-stacks from each lung sample.

Cell isolation and transcriptional profile analysis

Different P25 T cell subsets were sorted in a BD FACSAria II into: lung resident memory (L-RM, $CD69^+$), spleen effector memory (S-EM, $CD69^-CD62L^-$) from a pool of cells obtained from immunized mice (n = 20) 6 weeks after immunization. Effector P25 cells (S-eff) were obtained from mice that have been infected with PR8.p25 for 11 days. Following RNA extraction (QIAGEN RNeasy Mini), and DNase I (New England Biolabs) digestion, cDNA were prepared using Tetro cDNA synthesis kit (Bioline). Quantitative real-time PCR of *Klf2, S1pr1, Foxo1, Tbx21, Bcl-2, Bcl-xL,* and *Ifng* was performed with SensiFAST SYBR Hi-ROX mix and the following primers: 18s Fw GTAACCCGTTGAACCCCATT, Rv CCATCCAATCGGTAGTAGCG; Klf2 Fw-CTAAAGGCGCATCTGCGTA, Rv TAGTGGCGGGTAAGCTCGT; S1pr1 Fw CACAGGCAAGTTGAACATCG, Rv GGATGATGAAGCAGCAGATG; Foxo1 Fw TGTCAGGCTAAGAGTTAGTGAGCA, Rv GGGTGAAGGGCATCTTTG; Tbx21 Fw GCCAGGGAACCGCTTATATG, Rv GACGATCATCTGGGTCACATT; Bcl-2 Fw CCGGGAGAACAGGGTATGATAA, Rv CCCACTCGTAGCCCCTCTG; Bcl-xL Fw CACTGTGCGTGGAAAGCGTA, Rv AAAGTGTCCCAGCCGCC; IFNg Fw ACAATGAACGCTACACACTGCAT, Rv TGGCAGTAACAGCCAGAAACA. The threshold cycle of individual genes was normalized to the value of 18s rRNA (ΔC_T) for each cell population and gene expression calculated by the $2^{(-\Delta CT)}$ method.

497

498 Bacterial quantification

499 Bacterial quantification was performed by plating serial dilutions of lung
500 homogenates onto Middlebrook 7H11 supplemented with 10% oleic acid-albumin
501 enrichment (Difco) agar plates and culture for 3 weeks at 37 ^{o}C.

502

503 Statistical analysis

504 Data were analyzed using Student's *t* test when comparing two experimental groups
505 or ANOVA followed by Tukey post-test correction for more than 2 groups.
506 Differences with a value of $P < 0.05$ were considered statistically significant.

507

508 **Acknowledgments**

509 This work was supported by the National and Medical Research Council of Australia
510 through Project Grant APP1044343, and the Centre of Research Excellence in TB
511 Control (APP1043225), and the NSW Government through its infrastructure grant to
512 the Centenary Institute. H.M. was a recipient of Australia Award Scholarship from the
513 Australian Department of Foreign Affairs and Trade.

514

515 **Author contributions**

516 M.F., H.M. and L.L designed and performed experiments, and M.F wrote the
517 manuscript. Y.X. developed the rIAV vaccines under supervision of J.S.. F.S. assisted
518 with 2-photon microscopy experiments. M.P., C.F., P.B. and J.A.T. contributed to the
519 experimental design and provided intellectual input. W.B. was responsible for study
520 design, data interpretation and study supervision. All the authors contributed to the
521 editing of the manuscript.

Disclosure

No conflicts of interest to declare

References

1 WHO. Global Tuberculosis Report. (2017).

2 Fine, P. E. BCG: the challenge continues. *Scand J Infect Dis* **33**, 243-245 (2001).

3 Reiley, W. W. *et al.* Distinct functions of antigen-specific CD4 T cells during murine Mycobacterium tuberculosis infection. *Proceedings of the National Academy of Sciences of the United States of America* **107**, 19408-19413, doi:10.1073/pnas.1006298107 (2010).

4 Pawlowski, A., Jansson, M., Skold, M., Rottenberg, M. E. & Kallenius, G. Tuberculosis and HIV co-infection. *PLoS Pathog* **8**, e1002464, doi:10.1371/journal.ppat.1002464 (2012).

5 Tameris, M. D. *et al.* Safety and efficacy of MVA85A, a new tuberculosis vaccine, in infants previously vaccinated with BCG: a randomised, placebo-controlled phase 2b trial. *Lancet*, doi:10.1016/S0140-6736(13)60177-4 (2013).

6 Masopust, D., Vezys, V., Marzo, A. L. & Lefrancois, L. Preferential localization of effector memory cells in nonlymphoid tissue. *Science* **291**, 2413-2417, doi:10.1126/science.1058867 (2001).

7 Steinert, E. M. *et al.* Quantifying Memory CD8 T Cells Reveals Regionalization of Immunosurveillance. *Cell* **161**, 737-749, doi:10.1016/j.cell.2015.03.031 (2015).

8 Schenkel, J. M. & Masopust, D. Tissue-resident memory T cells. *Immunity* **41**, 886-897, doi:10.1016/j.immuni.2014.12.007 (2014).

9 Allende, M. L., Dreier, J. L., Mandala, S. & Proia, R. L. Expression of the sphingosine 1-phosphate receptor, S1P1, on T-cells controls thymic emigration. *J Biol Chem* **279**, 15396-15401, doi:10.1074/jbc.M314291200 (2004).

10 Carlson, C. M. *et al.* Kruppel-like factor 2 regulates thymocyte and T-cell migration. *Nature* **442**, 299-302, doi:10.1038/nature04882 (2006).

11 Mackay, L. K. *et al.* Cutting Edge: CD69 Interference with Sphingosine-1-Phosphate Receptor Function Regulates Peripheral T Cell Retention. *Journal of immunology* **194**, 2059-2063, doi:10.4049/jimmunol.1402256 (2015).

12 Wu, T. *et al.* Lung-resident memory CD8 T cells (TRM) are indispensable for optimal cross-protection against pulmonary virus infection. *J Leukoc Biol* **95**, 215-224, doi:10.1189/jlb.0313180 (2014).

13 Gebhardt, T. *et al.* Memory T cells in nonlymphoid tissue that provide enhanced local immunity during infection with herpes simplex virus. *Nat Immunol* **10**, 524-530, doi:10.1038/ni.1718 (2009).

14 Thom, J. T., Weber, T. C., Walton, S. M., Torti, N. & Oxenius, A. The Salivary Gland Acts as a Sink for Tissue-Resident Memory CD8(+) T Cells, Facilitating Protection from Local Cytomegalovirus Infection. *Cell Rep* **13**, 1125-1136, doi:10.1016/j.celrep.2015.09.082 (2015).

15 Sheridan, B. S. *et al.* Oral infection drives a distinct population of intestinal resident memory CD8(+) T cells with enhanced protective function. *Immunity* **40**, 747-757, doi:10.1016/j.immuni.2014.03.007 (2014).

16 Fernandez-Ruiz, D. *et al.* Liver-Resident Memory CD8+ T Cells Form a Front-Line Defense against Malaria Liver-Stage Infection. *Immunity* **45**, 889-902, doi:10.1016/j.immuni.2016.08.011 (2016).

17 Turner, D. L. *et al.* Lung niches for the generation and maintenance of tissue-resident memory T cells. *Mucosal immunology* **7**, 501-510, doi:10.1038/mi.2013.67 (2014).

18 Strutt, T. M. *et al.* IL-15 supports the generation of protective lung-resident memory CD4 T cells. *Mucosal Immunol*, doi:10.1038/mi.2017.101 (2017).

19 Oja, A. E. *et al.* Trigger-happy resident memory CD4(+) T cells inhabit the human lungs. *Mucosal Immunol*, doi:10.1038/mi.2017.94 (2017).

20 Florido, M. *et al.* Epitope-specific CD4+, but not CD8+, T-cell responses induced by recombinant influenza A viruses protect against Mycobacterium tuberculosis infection. *European journal of immunology* **45**, 780-793, doi:10.1002/eji.201444954 (2015).

21 Anderson, K. G. *et al.* Intravascular staining for discrimination of vascular and tissue leukocytes. *Nature protocols* **9**, 209-222, doi:10.1038/nprot.2014.005 (2014).

22 Kerdiles, Y. M. *et al.* Foxo1 links homing and survival of naive T cells by regulating L-selectin, CCR7 and interleukin 7 receptor. *Nat Immunol* **10**, 176-184, doi:10.1038/ni.1689 (2009).

23 Chiba, K. *et al.* Fingolimod (FTY720), sphingosine 1-phosphate receptor modulator, shows superior efficacy as compared with interferon-beta in mouse experimental autoimmune encephalomyelitis. *Int Immunopharmacol* **11**, 366-372, doi:10.1016/j.intimp.2010.10.005 (2011).

24 Morris, M. A. *et al.* Transient T cell accumulation in lymph nodes and sustained lymphopenia in mice treated with FTY720. *Eur J Immunol* **35**, 3570-3580, doi:10.1002/eji.200526218 (2005).

25 Srivastava, S. & Ernst, J. D. Cutting edge: Direct recognition of infected cells by CD4 T cells is required for control of intracellular Mycobacterium tuberculosis in vivo. *J Immunol* **191**, 1016-1020, doi:10.4049/jimmunol.1301236 (2013).

26 Sakai, S. *et al.* Cutting edge: control of Mycobacterium tuberculosis infection by a subset of lung parenchyma-homing CD4 T cells. *Journal of immunology* **192**, 2965-2969, doi:10.4049/jimmunol.1400019 (2014).

27 Connor, L. M. *et al.* A key role for lung-resident memory lymphocytes in protective immune responses after BCG vaccination. *Eur J Immunol* **40**, 2482-2492, doi:10.1002/eji.200940279 (2010).

28 Perdomo, C. *et al.* Mucosal BCG Vaccination Induces Protective Lung-Resident Memory T Cell Populations against Tuberculosis. *MBio* **7**, doi:10.1128/mBio.01686-16 (2016).

29 Turner, D. L. & Farber, D. L. Mucosal resident memory CD4 T cells in protection and immunopathology. *Frontiers in immunology* **5**, 331, doi:10.3389/fimmu.2014.00331 (2014).

30 Horvath, C. N., Shaler, C. R., Jeyanathan, M., Zganiacz, A. & Xing, Z. Mechanisms of delayed anti-tuberculosis protection in the lung of parenteral BCG-vaccinated hosts: a critical role of airway luminal T cells. *Mucosal Immunol* **5**, 420-431, doi:10.1038/mi.2012.19 (2012).

31 Casey, K. A. *et al.* Antigen-independent differentiation and maintenance of effector-like resident memory T cells in tissues. *J Immunol* **188**, 4866-4875, doi:10.4049/jimmunol.1200402 (2012).

32 Teijaro, J. R. *et al.* Cutting edge: Tissue-retentive lung memory CD4 T cells mediate optimal protection to respiratory virus infection. *J Immunol* **187**, 5510-5514, doi:10.4049/jimmunol.1102243 (2011).

33 Mackay, L. K. *et al.* The developmental pathway for CD103(+)CD8+ tissue-resident memory T cells of skin. *Nature immunology* **14**, 1294-1301, doi:10.1038/ni.2744 (2013).

34 Skon, C. N. *et al.* Transcriptional downregulation of S1pr1 is required for the establishment of resident memory CD8+ T cells. *Nat Immunol* **14**, 1285-1293, doi:10.1038/ni.2745 (2013).

35 Huang, H. & Tindall, D. J. Regulation of FOXO protein stability via ubiquitination and proteasome degradation. *Biochim Biophys Acta* **1813**, 1961-1964, doi:10.1016/j.bbamcr.2011.01.007 (2011).

36 Zens, K. D., Chen, J. K. & Farber, D. L. Vaccine-generated lung tissue-resident memory T cells provide heterosubtypic protection to influenza infection. *JCI Insight* **1**, doi:10.1172/jci.insight.85832 (2016).

37 Walker, K. B. *et al.* Novel approaches to preclinical research and TB vaccine development. *Tuberculosis (Edinb)* **99 Suppl 1**, S12-15, doi:10.1016/j.tube.2016.05.012 (2016).

38 Hoffmann, E., Krauss, S., Perez, D., Webby, R. & Webster, R. G. Eight-plasmid system for rapid generation of influenza virus vaccines. *Vaccine* **20**, 3165-3170 (2002).

641 39 Cukalac, T. *et al.* Narrowed TCR diversity for immunised mice challenged
642 with recombinant influenza A-HIV Env(311-320) virus. *Vaccine* **27**, 6755-
643 6761, doi:10.1016/j.vaccine.2009.08.079 (2009).
644
645

Figure Legends

Figure 1. Pulmonary, but not systemic, immunization with PR8.p25 induces p25 $CD4^+$ T cells in the lung

Fifty thousand $CD45.1^+$ P25 Tg splenic cells were adoptively transferred into naïve recipient C57Bl/6 one day prior to immunization intranasally with 20 pfu or intraperitoneally with $5x10^4$ pfu of PR8.p25. IFNγ responses in the lung (A) and in the spleen (B) against influenza A virus NP and *M. tuberculosis* Ag85B P25 epitopes, 3 weeks after delivery of PR8.p25 intraperitoneally (black) or intranasally (grey) measured by IFNγ ELISPOT. Number of P25 $CD4^+$ T cells in the BAL (C), lung (D) and spleen (E) determined by flow cytometry. Data presented as mean ± SEM (n=4).

Figure 2. Intranasal immunization with PR8.p25 induces the persistence of $CD69^+$ $CD11a^+$ p25 $CD4^+$ T cells in the lung parenchyma

Fifty thousand $CD45.1^+$ P25 or GFP-P25 Tg splenic cells were adoptively transferred into naïve recipient C57Bl/6 mice one day prior to immunization intranasally with 20 pfu PR8.p25. (A) Kinetics of the transferred $CD45.1^+$ P25 $CD4^+$ T cells in the lung after immunization with PR8.p25. (B) Expression of CD69 and CD103 by the P25 CD4 T cells. (C) Intravascular staining showing the CD45-unlabeled GFP-P25 T cells located in the lung parenchyma (quadrant I) and the vascular CD45-labeled GFP-P25 T cells (quadrant II), (D) CD69 expression profile in parenchymal (blue) vs. vascular (red) GFP-P25 T cells, (E) expression of CD69 and CD11a and (F) CD44 and CD62L in GFP-P25 parenchymal cells and (E) numbers of parenchymal GFP-P25 cells expressing CD69 and CD11a at 8 weeks after immunization with PR8.p25. The data are representative of 1 of 2 independent experiments and are presented as mean ± SEM (n=3-5).

Figure 3. Detection of GFP-P25 CD4$^+$ T cell at 6 weeks after immunization with PR8.p25 using 2-photon microscopy

GFP-P25 cells were detected in an *ex vivo* lung (A), and their extravascular location confirmed after injection of WGA-A594 that allows visualization of the vasculature (B). (C) Detection of GFP-P25 cells deeper into the tissue after clearing of the lung with RapiClear1.52. (D) Comparison of the frequency of GFP-P25 cells in the lung as determined by flow cytometry and by 2-P microscopy 8 weeks after immunization with PR8.p25.

Figure 4. P25 CD4$^+$ T cells induced by PR8.p25 immunization have the transcriptional profile of tissue resident memory cells

Fifty thousand CD45.1$^+$ P25 Tg splenic cells were adoptively transferred into naïve recipient C57Bl/6 mice one day prior to immunization intranasally with 20 pfu PR8.p25. Lung CD69$^+$ P25 CD4$^+$ T cells (L-RM) and splenic CD69-CD62Llo (S-EM) were sorted from mice immunized with PR8.p25 6 weeks before (n=12-20). P25 CD4$^+$ effector cells (S-eff) were sorted from the lungs of mice 11 days after immunization with PR8.p25. Quantitative real-time PCR analysis of (A*) klf2, s1pr1, foxo1, tbx21, ifng* and (B) *bcl*-2 and *bcl-xl* mRNA in P25 cells sorted from the spleens and lungs of naïve and PR8-p25 immunized mice. The representative figure shows the results from one of two independent experiments.

Figure 5. Effect of FTY720 treatment on CD4$^+$ T cells after infection with *M. tuberculosis*.

Fifty thousand GFP-P25 Tg splenic cells were adoptively transferred into naïve recipient C57Bl/6 mice one day prior to intranasal immunization with 5x10^4 pfu X31-p25. Six weeks after immunization, both naïve and immunized mice were treated with FTY720, 1 mg/kg by i.p. daily for 20 days and challenged with *M. tuberculosis* at day 3 of treatment. CD4$^+$ T cell populations were analyzed and compared with those of naïve and immunized mice infected with *M. tuberculosis* but not treated with FTY720. (A) Diagram of the experimental plan. The number of CD4$^+$ T cells present in the blood (B), mediastinal lymph node (C), lung parenchyma (D), and lung vasculature (E) at 17 days post infection. (F) Number of GFP-P25 Tg CD4$^+$ T cells, (G) pie charts representing the proportion of the different subset populations of GFP-P25 CD4$^+$ T cells based on the surface markers CD69, CD11a, CD62L and KLRG1 and (H) number of CD69$^+$CD11a$^+$CD62L^{lo}KLRG1$^-$ GFP-P25 CD4$^+$ T cells present in the lung parenchyma at day 17 and 28 post *M. tuberculosis* infection. Results in B-F and H are shown as mean ± SD (n=5-7). Results in G were obtained using the FlowJo bolean gating tool. The representative figure shows the results from one of two independent experiments. **** $p < 0.0001$, *** $p < 0.001$, ** $p < 0.01$, * $p< 0.05$, ANOVA followed by Tukey post-test correction.

Figure 6. CD4$^+$ T cell cytokine production in *M. tuberculosis* infected lungs after FTY720 treatment.

Naïve and mice immunized with X31-p25 were treated with FTY720 and challenged with *M. tuberculosis* as in Fig 5. Lung cells were stimulated with p25 peptide and the cytokine production assessed by ICS assay. (A) Frequency of cytokine producing

720 $CD4^+$ T cells in the lung parenchyma at 17 days post *M. tuberculosis* infection.
721 Cytokine production by GFP-P25 $CD4^+$ T cells in the lung parenchyma at 17 days (B)
722 and 28 days (C) post *M. tuberculosis* infection. Pie charts represent the relative
723 proportions of p25-specific $CD4^+$ T cells expressing the possible combinations of
724 IFNγ, TNF and IL-2. Analysis of the different cytokine producing subsets was
725 performed by flow cytometry using FlowJo Bolean gating tool. Results are shown as
726 mean + SD (n≥5) and are from one of two independent experiments. ****p<0.0001,
727 ***p<0.001, **p<0.01, *p<0.05, ANOVA followed by Tukey post-test correction.
728
729 **Figure 7. PR8.p25-induced lung-resident $CD4^+$ T cells confer protection against**
730 ***M. tuberculosis* following depletion of circulating T cells.**
731 Naïve and mice immunized with X31-p25 were treated with FTY720 and challenged
732 with *M. tuberculosis* as in Fig 5. Mycobacterial loads in the lungs of mice were
733 determined at 17 (A) and 28 days (B) after infection with *M. tuberculosis.* The data
734 are shown with symbols for individual animals and as mean ± SEM (n=6) and are
735 representative of results from one of two independent experiments. **** p <
736 0.0001,***p<0.001, **p<0.01, ANOVA followed by Tukey post-test correction.
737

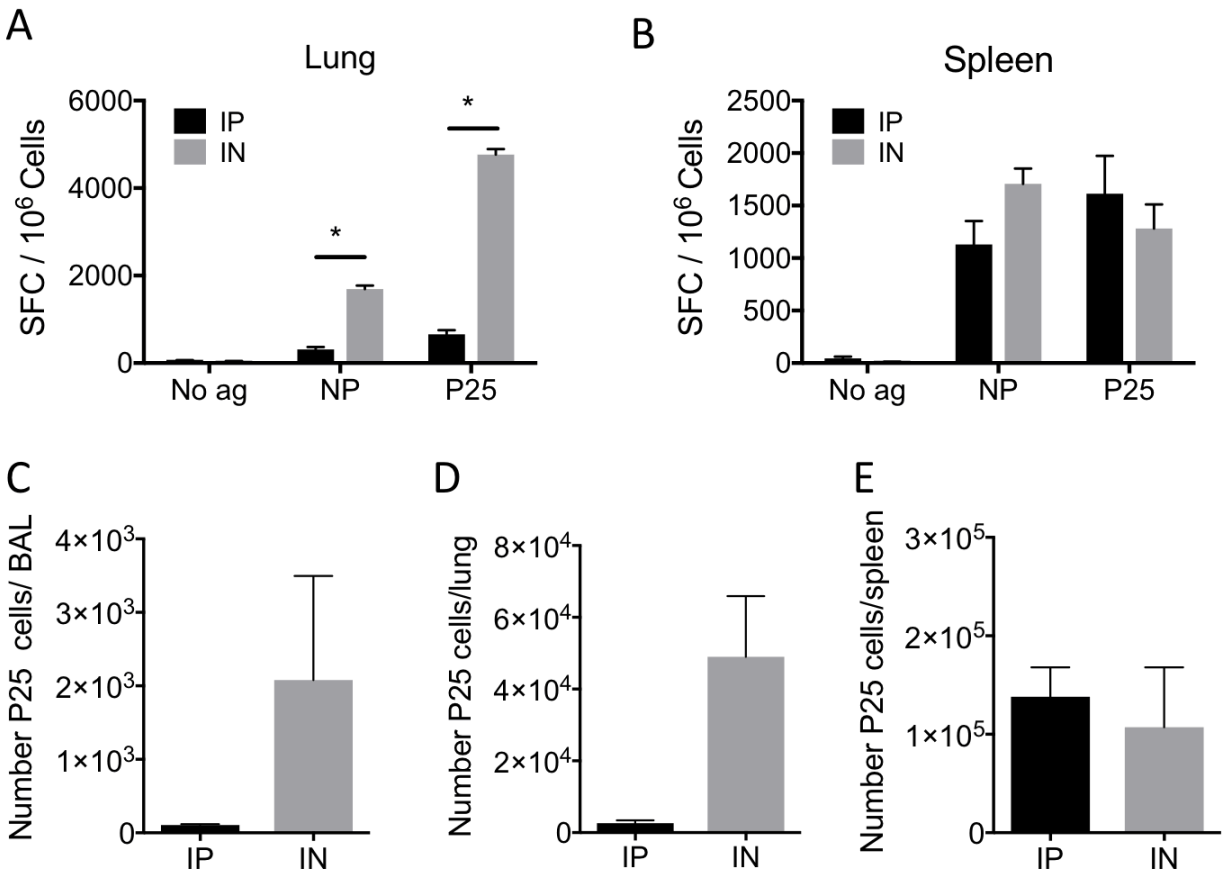
A
Lung
SFC / 10^6 Cells
6000
4000
2000
0
IP
IN
*
*
No ag
NP
P25
B
Spleen
SFC / 10^6 Cells
2500
2000
1500
1000
500
0
IP
IN
No ag
NP
P25
C
Number P25 cells/ BAL
4×10^3
3×10^3
2×10^3
1×10^3
0
IP
IN
D
Number P25 cells/lung
8×10^4
6×10^4
4×10^4
2×10^4
0
IP
IN
E
Number P25 cells/spleen
3×10^5
2×10^5
1×10^5
0
IP
IN

Figure 1

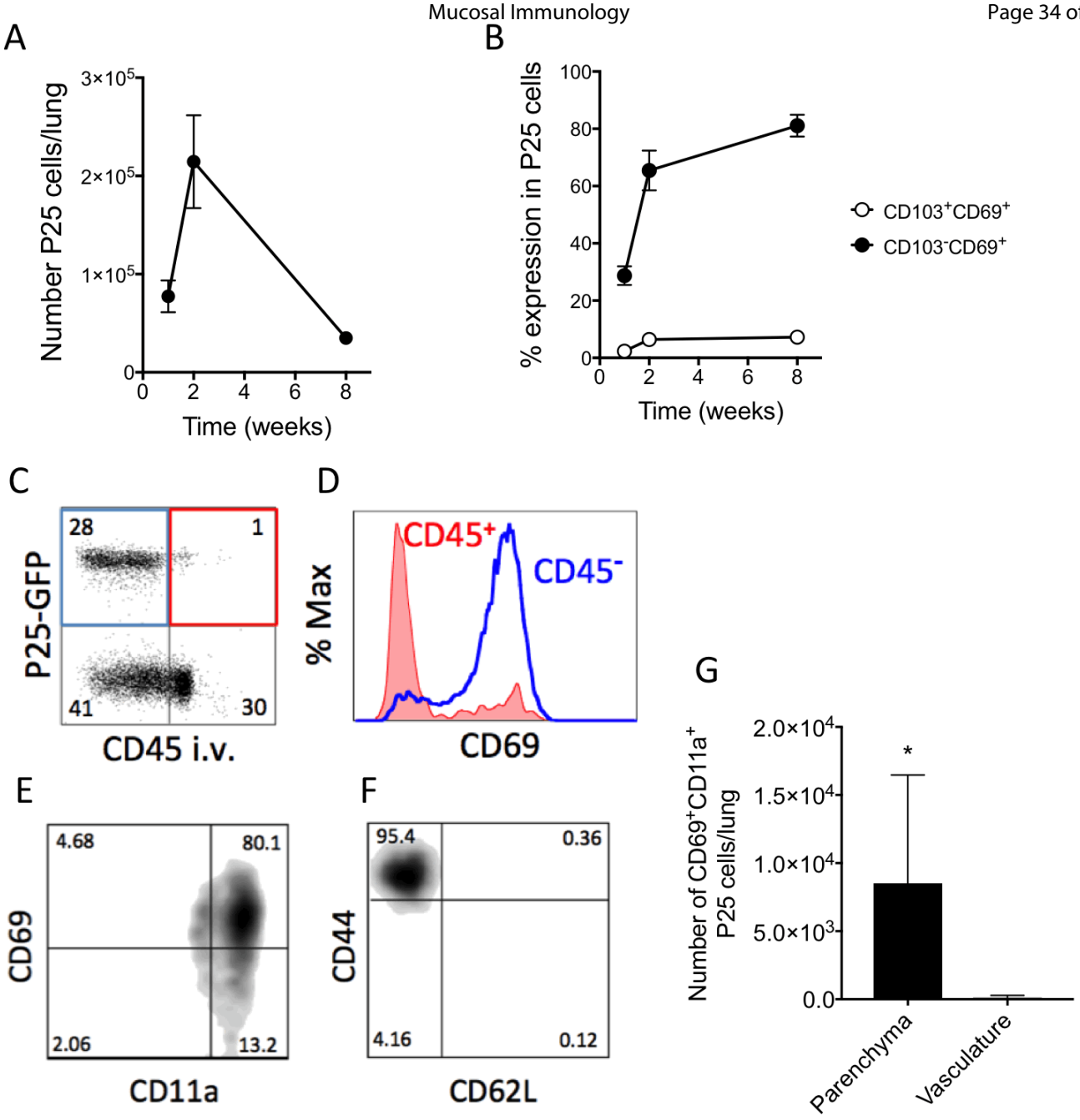
A
Number P25 cells/lung
3×10^5
2×10^5
1×10^5
0
0 2 4 6 8
Time (weeks)
B
% expression in P25 cells
100
80
60
40
20
0
0 2 4 6 8
Time (weeks)
CD103+CD69+
CD103-CD69+
C
P25-GFP
28
1
41
30
CD45 i.v.
D
% Max
CD45+
CD45-
CD69
E
CD69
4.68
80.1
2.06
13.2
CD11a
F
CD44
95.4
0.36
4.16
0.12
CD62L
G
Number of CD69+CD11a+ P25 cells/lung
2.0×10^4
1.5×10^4
1.0×10^4
5.0×10^3
0.0
*
Parenchyma
Vasculature

Figure 2

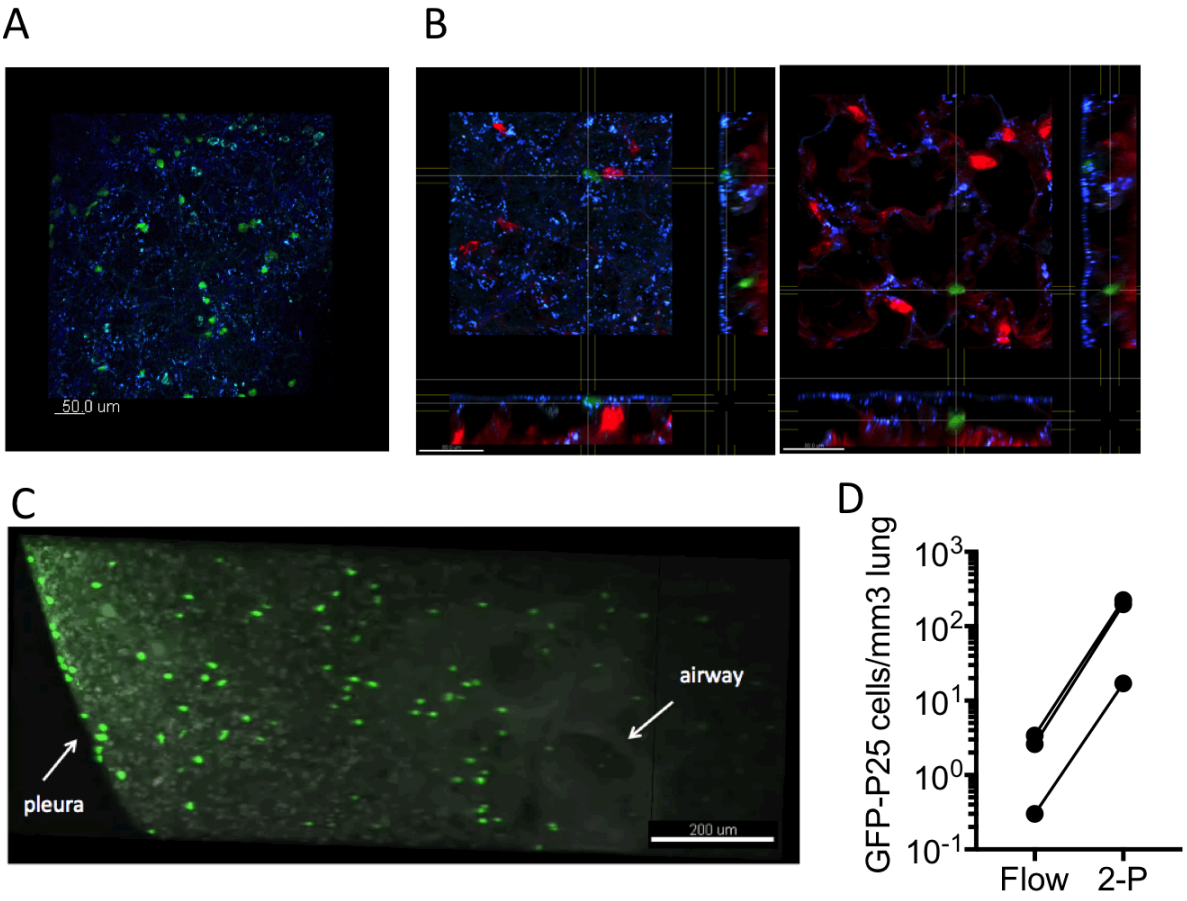
A
B
50.0 um
C
airway
pleura
200 um
D
GFP-P25 cells/mm3 lung
10^3
10^2
10^1
10^0
10^{-1}
Flow
2-P

Figure 3

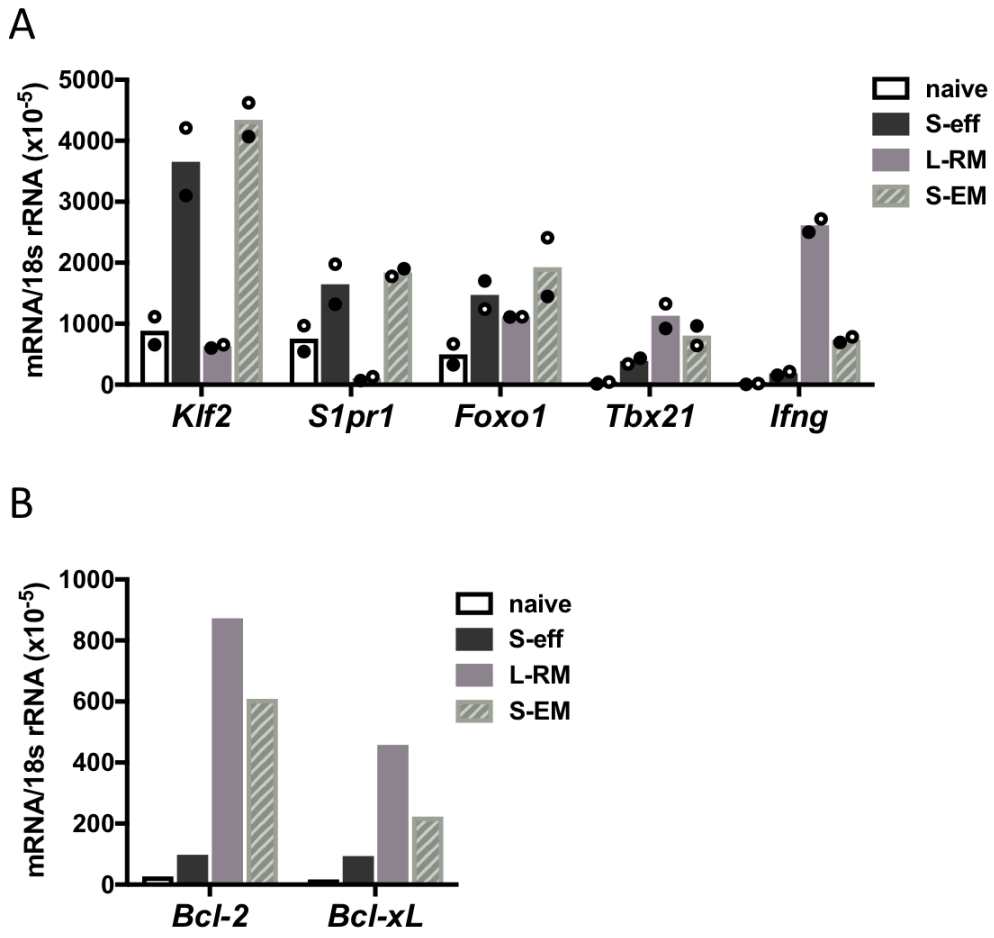
A
mRNA/18s rRNA (x10-5)
5000
4000
3000
2000
1000
0
naive
S-eff
L-RM
S-EM
Klf2
S1pr1
Foxo1
Tbx21
Ifng
B
mRNA/18s rRNA (x10-5)
1000
800
600
400
200
0
naive
S-eff
L-RM
S-EM
Bcl-2
Bcl-xL

Figure 4.

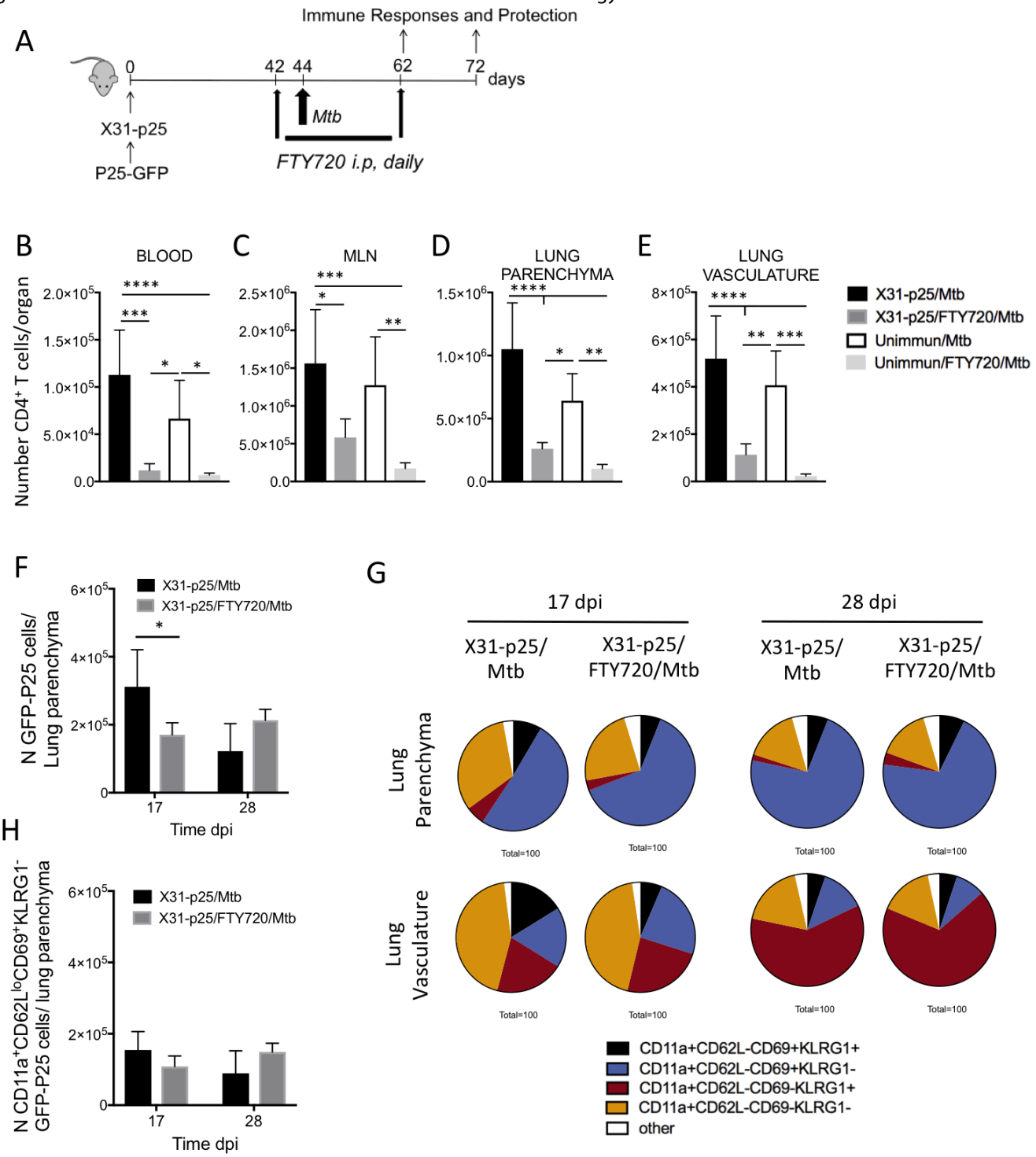
A
Immune Responses and Protection
0
42 44
62
72
days
X31-p25
P25-GFP
Mtb
FTY720 i.p, daily
B
BLOOD
C
MLN
D
LUNG PARENCHYMA
E
LUNG VASCULATURE
Number CD4+ T cells/organ
X31-p25/Mtb
X31-p25/FTY720/Mtb
Unimmun/Mtb
Unimmun/FTY720/Mtb
F
N GFP-P25 cells/ Lung parenchyma
Time dpi
G
17 dpi
28 dpi
X31-p25/ Mtb
X31-p25/ FTY720/Mtb
Lung Parenchyma
Lung Vasculature
Total=100
CD11a+CD62L-CD69+KLRG1+
CD11a+CD62L-CD69+KLRG1-
CD11a+CD62L-CD69-KLRG1+
CD11a+CD62L-CD69-KLRG1-
other
H
N CD11a+CD62LloCD69+KLRG1- GFP-P25 cells/ lung parenchyma
Time dpi

Fig 5

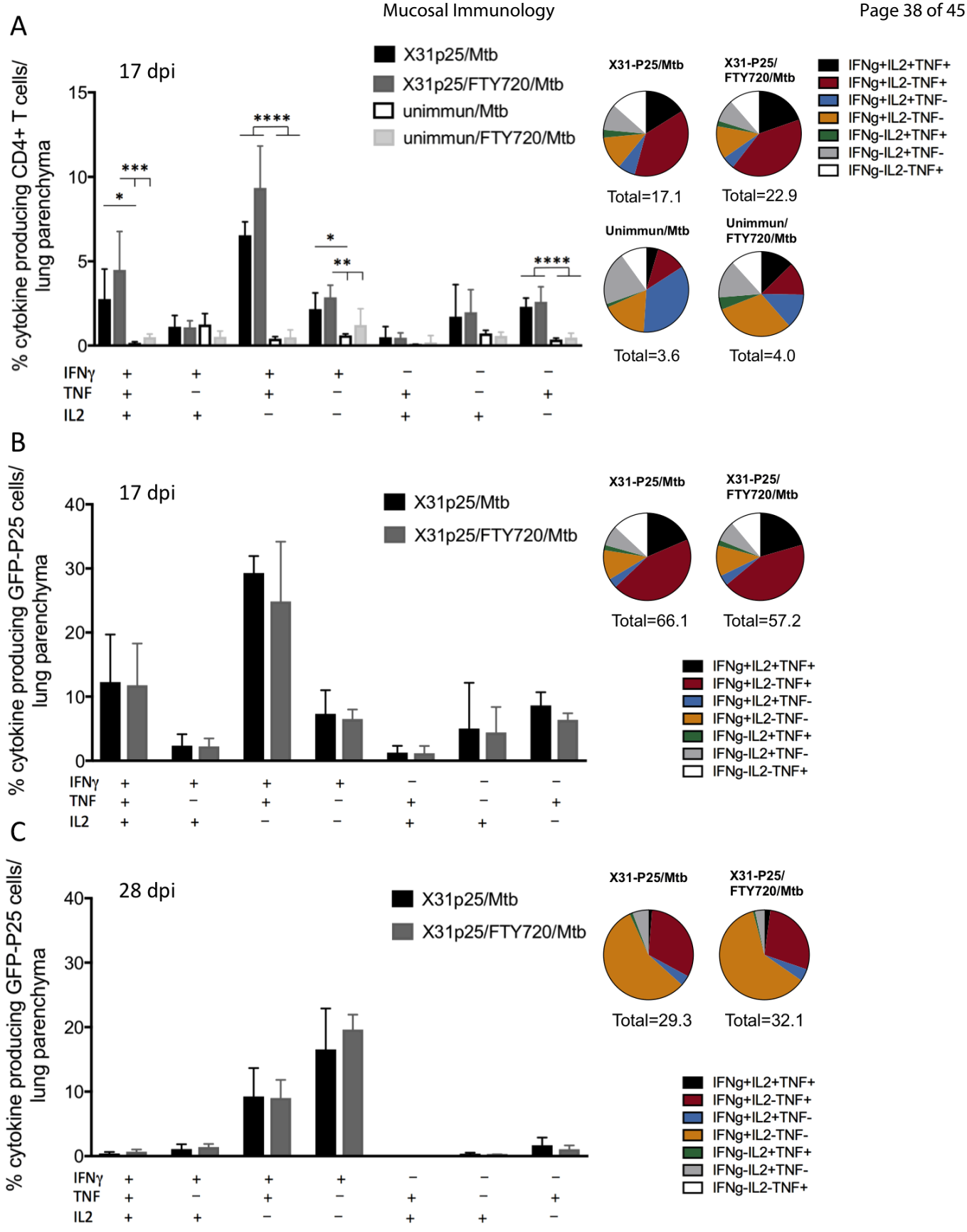
A
17 dpi
X31p25/Mtb
X31p25/FTY720/Mtb
unimmun/Mtb
unimmun/FTY720/Mtb
% cytokine producing CD4+ T cells/ lung parenchyma
IFNγ
TNF
IL2
X31-P25/Mtb
X31-P25/ FTY720/Mtb
Unimmun/Mtb
Unimmun/ FTY720/Mtb
Total=17.1
Total=22.9
Total=3.6
Total=4.0
IFNg+IL2+TNF+
IFNg+IL2-TNF+
IFNg+IL2+TNF-
IFNg+IL2-TNF-
IFNg-IL2+TNF+
IFNg-IL2+TNF-
IFNg-IL2-TNF+
B
17 dpi
X31p25/Mtb
X31p25/FTY720/Mtb
% cytokine producing GFP-P25 cells/ lung parenchyma
Total=66.1
Total=57.2
C
28 dpi
X31p25/Mtb
X31p25/FTY720/Mtb
% cytokine producing GFP-P25 cells/ lung parenchyma
Total=29.3
Total=32.1

Fig 6

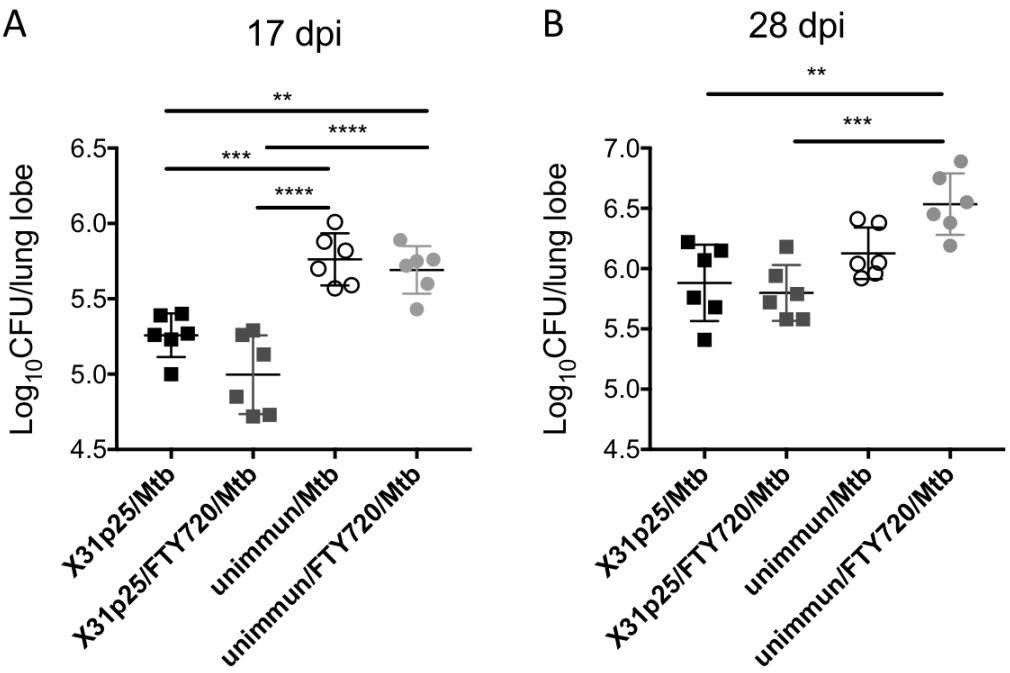
A
17 dpi
**
****
***
****
6.5
6.0
5.5
5.0
4.5
Log10CFU/lung lobe
X31p25/Mtb
X31p25/FTY720/Mtb
unimmun/Mtb
unimmun/FTY720/Mtb
B
28 dpi
**
***
7.0
6.5
6.0
5.5
5.0
4.5
Log10CFU/lung lobe
X31p25/Mtb
X31p25/FTY720/Mtb
unimmun/Mtb
unimmun/FTY720/Mtb

Fig 7.

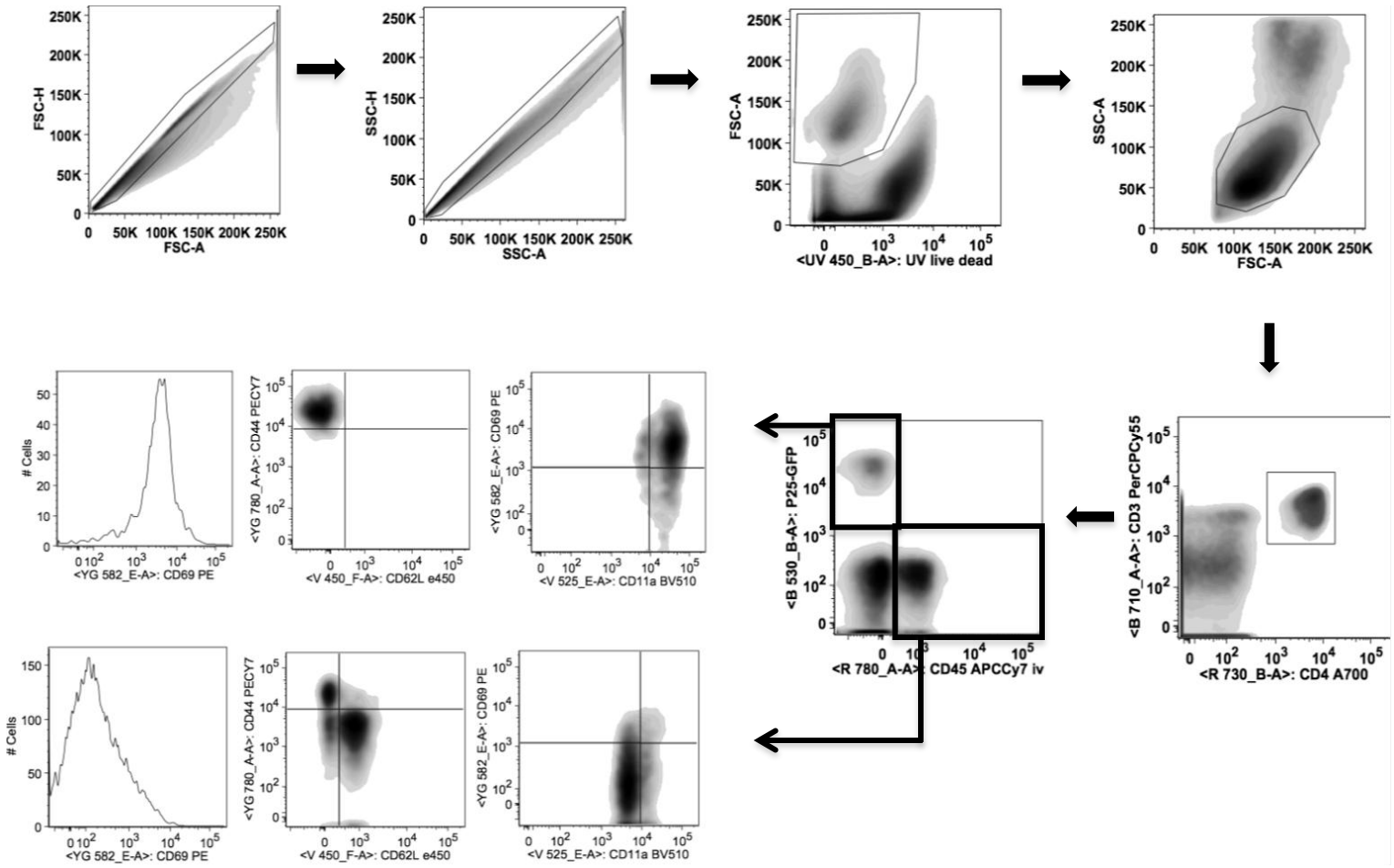

Supplementary Figure 1: Gating strategy for surface markers analysis. After exclusion of duplets and dead cells, lymphocytes were selected based on FSC vs SSC plots and CD3+CD4+ T cell population gated. The P25-GFP and other CD4 T cells were then discriminated between vascular (CD45+) and parenchymal (CD45-) based on IVS staining before analysis of TRM markers.

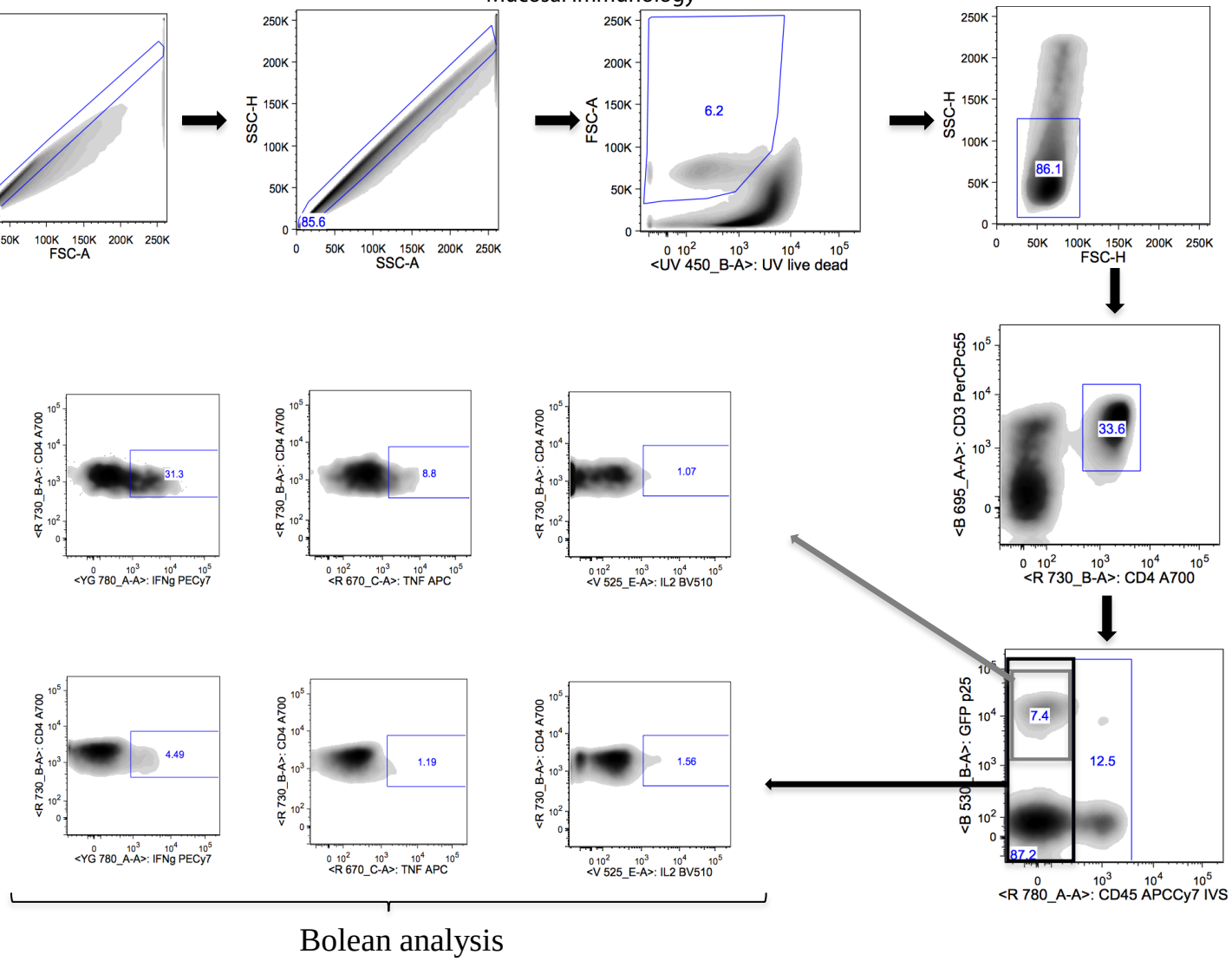

Supplementary Figure 2: Gating strategy for cytokine production analysis. After exclusion of duplets and dead cells, lymphocytes were selected based on FSC vs SSC plots and CD3+CD4+ T cell population gated. The P25-GFP and other CD4 T cells were then discriminated between vascular (CD45+) and parenchymal (CD45-) based on IVS staining before analysis of cytokine production by bolean gating.

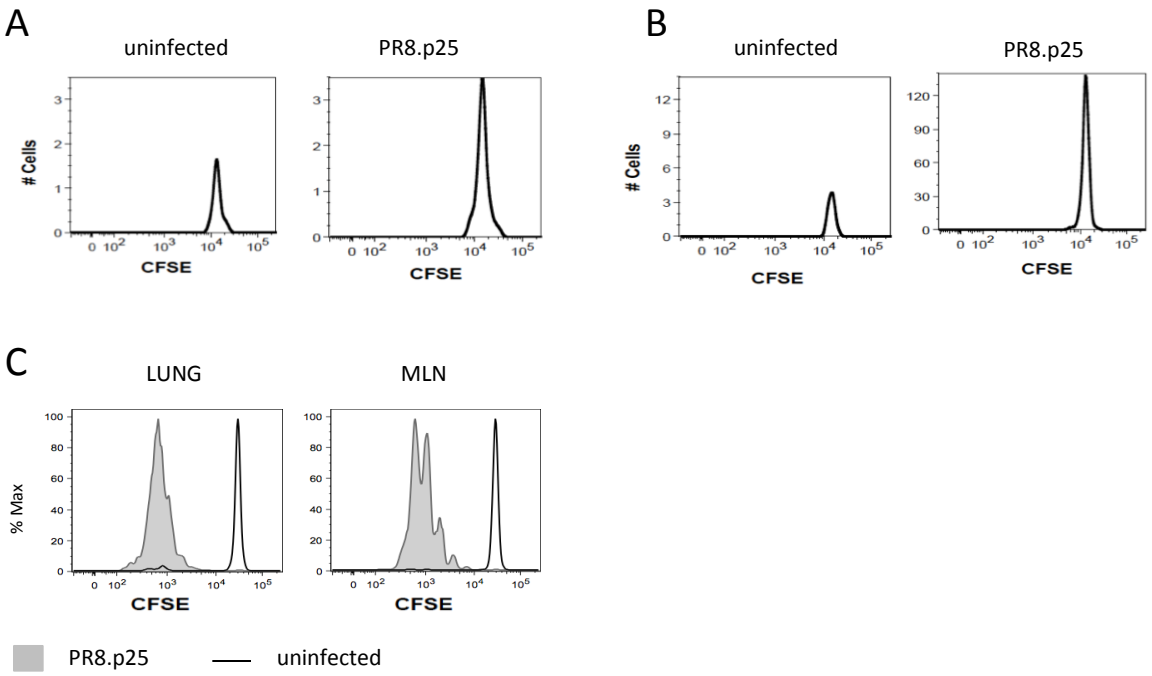

Supplementary Figure 3: 5x10^5 CFSE labelled CD45.1+ P25 Tg were adoptively transferred into unimmunized mice and mice immunized i.n. with PR8.p25 6 weeks before. The CFSE profile of transferred CD45.1 P25 CD4 T cells was analyzed in the lung (A) and MLN (B) 3 days after adoptive transfer. (C) CFSE profiles when the P25 Tg cells were transferred at day 5 after PR8.p25 immunization (grey tinted) or unimmunized mice (black line). The results are representative of 1 out of 2 experiments and are presented as mean±SE (n=3-5)

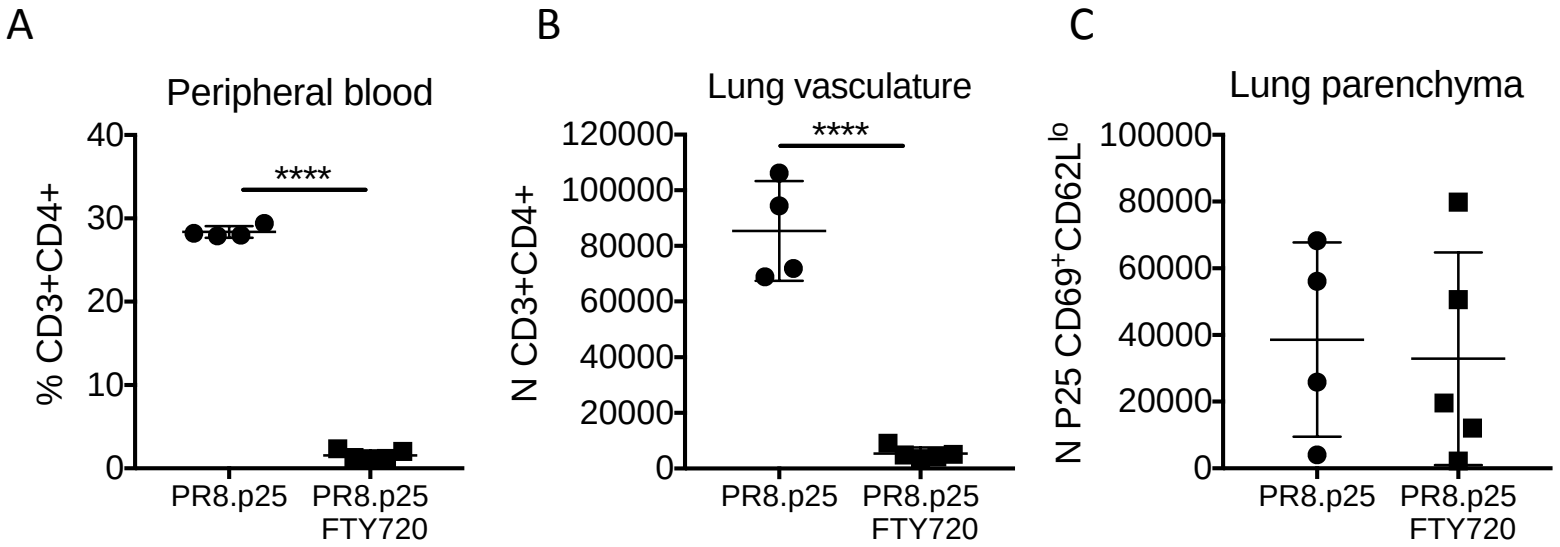

Supplementary Figure 4: (A) Percentage of circulation of CD3+ CD4+ T cells present in the peripheral blood, (B) number of CD3+ CD4+ T cells present in the lung vasculature and (C) number of CD69+CD62Llo P25 CD4+ T cells present in the lung parenchyma of mice immunized with PR8.p25 6 weeks prior to treatment during 20 days with FTY (circles) or control non FTY treated mice (squares).

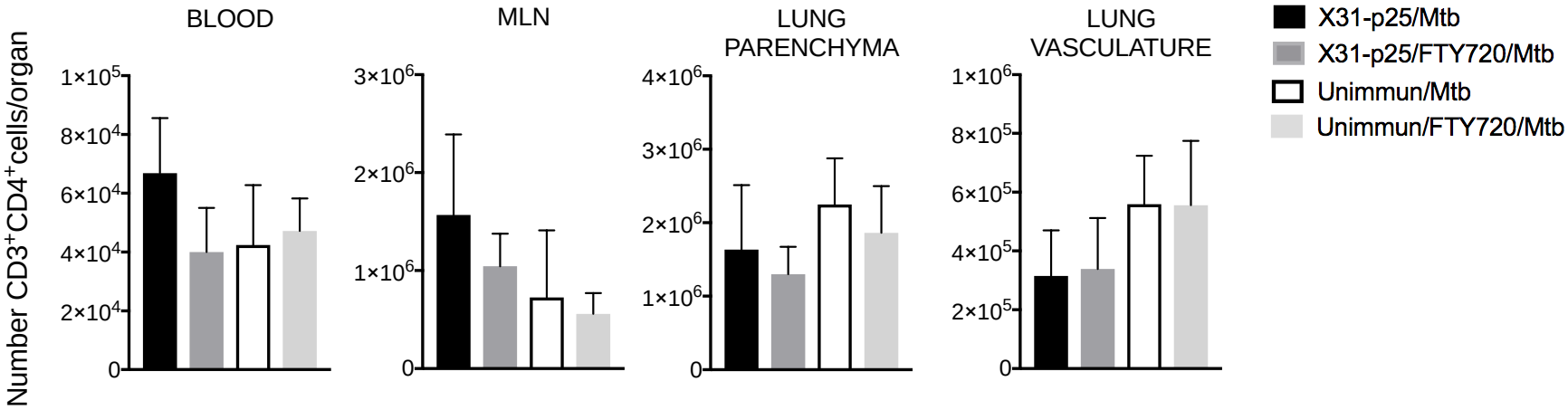

Supplementary Figure 5: Naïve and mice immunized with X31-p25 were treated with fingolimod and challenged with *Mtb* as in Fig 5 A. The number of $CD4^+$ T cells present in the blood (B), mediastinal lymph node (C), lung parenchyma (D) and lung vasculature (E) at day 28 days post-*Mtb* infection in unimmunized and PR8.p25 immunized mice, treated and not treated with FTY720. Results are shown as mean + SD (n≥5). The representative figure shows the results from one out of two independent experiments.

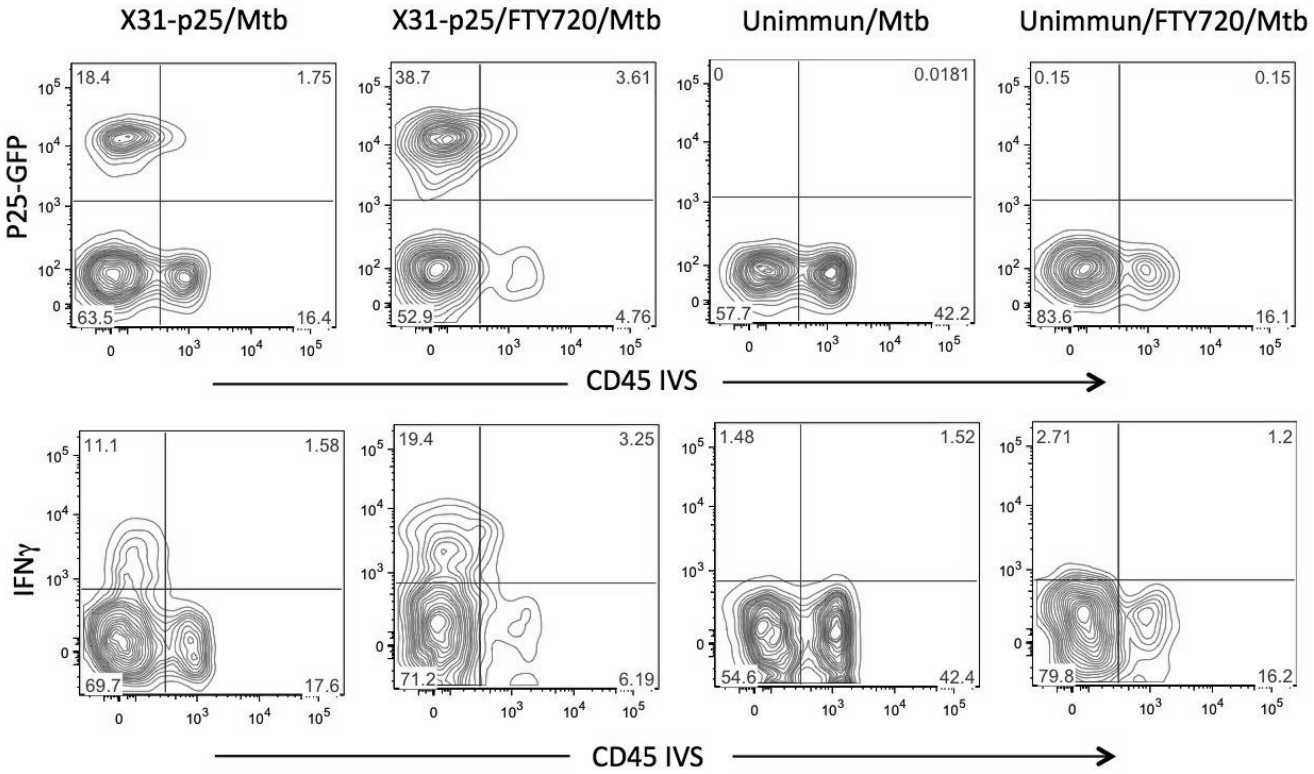

Supplementary Figure 6: Naïve and mice immunized with X31-p25 were treated with fingolimod and challenged with *Mtb* as in Fig 5 A. Representative dot-plots of intravascular staining in unimmunized and PR8.p25 immunized mice, treated and not treated with FTY720 at day 17 post-*Mtb* infection.

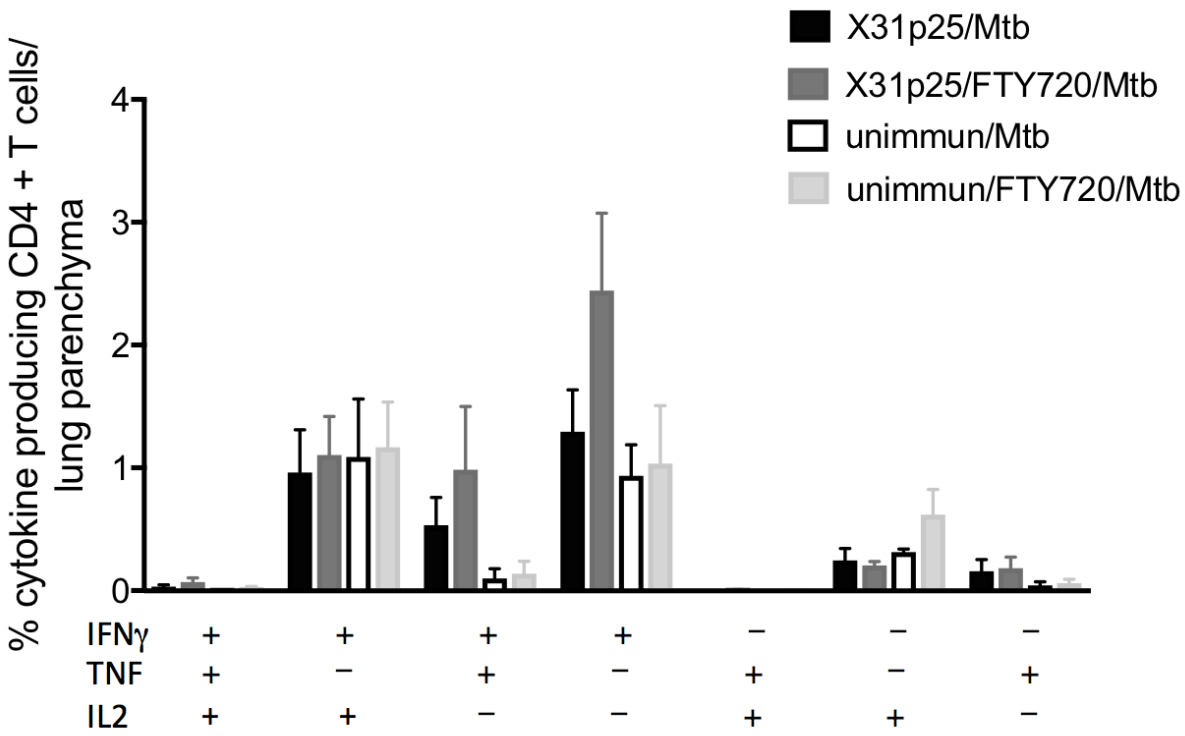

Supplementary Figure 7: Naïve and mice immunized with X31-p25 were treated with FTY720 and challenged with *Mtb* as in Fig 5 A. Lung cells were recalled with p25 peptide and the cytokine production assessed by ICS assay. Frequency of cytokine producing CD4+ T cells in the lung parenchyma at 28 days post-*Mtb* infection. Results are shown as mean + SD (n≥5). The representative figure shows the results from one out of two independent experiments.